High-energy dispersion anomaly induced by the charge modulation in high-T_c superconductors

T. Zhou[1] and Z. D. Wang[1,2]

[1]*Department of Physics and Center of Theoretical and Computational Physics, The University of Hong Kong, Pokfulam Road, Hong Kong, China*

[2]*National Laboratory of Solid State Microstructures, Nanjing University, Nanjing 210093, China*

(Received 8 January 2007; revised manuscript received 18 March 2007; published 4 May 2007)

We propose that the presence of a rotationally symmetric charge modulation in high-T_c superconductors is able to account for an anomalous quasiparticle dispersion revealed recently by angle-resolved photoemission spectroscopy (ARPES) experiments. We elaborate that the nodal quasiparticle is well defined at low energies, while the dispersion breaks up at the energy E_1 and reappears at the energy E_2. Our results are in agreement with both the ARPES and scanning tunneling microscopy experiments.

DOI: 10.1103/PhysRevB.75.184506 PACS number(s): 74.25.Jb, 74.20.Fg

Recently, scanning tunneling microscopy (STM) experiments have been performed to search for hidden electronic orders in high-T_c superconductors. A checkerboard pattern with the spatial four-unit-cell modulation for the local density of states was first seen around magnetic vortex cores in slightly overdoped samples by Hoffman *et al.*[1] This kind of modulation pattern was also reported in later STM experiments, in zero field and in both the superconducting (SC) and normal states.[2–6] In addition, the Fourier transform of the STM (FT-STM) spectra reveals four nondispersive peaks around $(\pm 2\pi/4, 0)$ and $(0, \pm 2\pi/4)$ in the normal[2] and SC states.[3–6] All of these experimental results indicate that a kind of charge modulation with a characteristic wave vector in the CuO bond direction of $q \sim 2\pi/4$ exists likely in high-T_c superconductors.[7]

On the other hand, an intriguing anomalous quasiparticle dispersion was very recently observed in angle-resolved photoemission spectroscopy (ARPES) experiments,[8–14] i.e., a well-defined nodal quasiparticle dispersion is broken down between the two higher energies E_1 and E_2, which drops in a waterfall fashion with a very low spectral weight. Below E_2, the quasiparticle dispersion reappears and disperses toward the zero center. These anomalous features were observed in several families of cuprates, in under-, optimal-, as well as overdoped samples, and below or above the SC transition temperature. In hole-doped samples, the energies E_1 and E_2 are around 0.35 and 0.8 eV, respectively, while in the electron-doped samples, the corresponding energies are found to be significantly larger with E_1 being around 0.6 eV.[13,14] The mechanism of these features is still unclear while it should be independent of the SC order. In addition, similar anomalous higher-energy features were also observed in the insulating cuprate $Ca_2CuO_2Cl_2$.[15] Thus, the mode coupling picture[16] can hardly account for these higher-energy behaviors because it is expected to happen only in metallic systems. Note that it was proposed before that the charge modulation may cause several other puzzling features seen in ARPES experiments.[17–19] Moreover, a connection between the ARPES and the FT-STM spectra was recently established[20,21] through the autocorrelation of the ARPES (AC-ARPES) spectra. Therefore, it is natural and significant to ask whether the above-mentioned anomalous dispersion observed in ARPES experiments can also be originated from the charge modulation, which has already been detected by the STM experiments. We here answer this question clearly by studying the spectral function and the FT-STM based on a simple phenomenological model including the charge modulation, though we note that a recent theory based on a new representation of the *t-J* model with two-band fermions was also proposed for the anomaly.[22]

At present, however, our knowledge on the origin and effects of the charge modulation is still far from complete. What the phase diagram of such an order is and whether it exists in all cuprate materials are still unclear.[17] In fact, the STM experiments are mostly carried out on the $Bi_2Sr_2CaCu_2O_{8+x}$ and $Ca_{2-x}Na_xCuO_2Cl_2$ samples, while a similar four-unit-cell structure was also found in the $YBa_2Cu_3O_y$ samples by diffuse x-ray scattering measurements.[23] On the other hand, it seems widely believed that the charge modulation may have the same physics as the stripe order,[17] which has been seen in the $La_{2-x}Sr_xCuO_4$ sample.[24] In addition, the stripe order is suggested to exist in various doping regions and to be the ground state of the cuprates.[25] Considering the above experimental and theoretical results, in this paper, we employ a phenomenological scenario that admits the existence of four-lattice-constant charge modulation to look into and elaborate its effect on the spectral function. The FT-STM spectra are also evaluated within our simple model and are compared with the STM experiments. We demonstrate that the charge modulation is able to naturally lead to the higher-energy anomaly in ARPES experiments and the nondispersive peaks in the FT-STM spectra. Considering the robustness of this higher-energy anomaly, our results suggest that the charge modulation be likely more robust in high-T_c superconductors.

We start with the following phenomenological Hamiltonian with a charge modulation being taken into account:

$$H = H_{BCS} + H_C, \tag{1}$$

where H_{BCS} is the BCS-type Hamiltonian given by

$$H_{BCS} = \sum_{\mathbf{k},\sigma} \varepsilon_{\mathbf{k}} c^{\dagger}_{\mathbf{k}\sigma} c_{\mathbf{k}\sigma} + \sum_{\mathbf{k}} (\Delta_{\mathbf{k}} c^{\dagger}_{\mathbf{k}\uparrow} c^{\dagger}_{-\mathbf{k}\downarrow} + \text{H.c.}), \tag{2}$$

where $\varepsilon_{\mathbf{k}} = -2t(\cos k_x + \cos k_y) - 4t' \cos k_x \cos k_y - \mu$, $\Delta_{\mathbf{k}}$ is the gap function, with $\Delta_{\mathbf{k}} = \Delta_0(\cos k_x - \cos k_y)/2$ for the *d*-wave

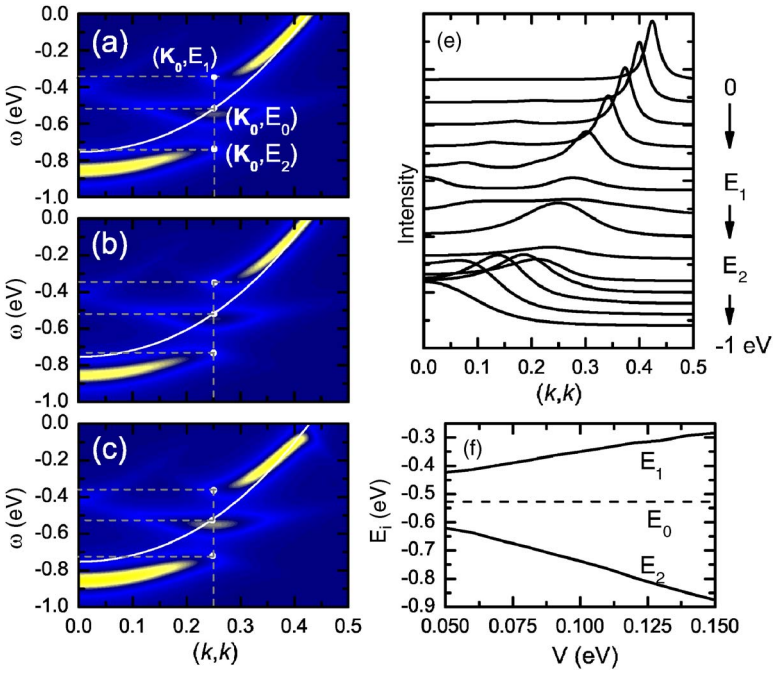

FIG. 1. (Color online) Panels (a), (b), and (c) are the intensity plots of the spectral function as functions of the momentum and energy in the normal state, d-wave SC state, and isotropic s-wave SC state ($\Delta_{\mathbf{k}} \equiv \Delta_0 = 50$ meV), respectively. The solid lines represent the bare dispersions $\varepsilon_{\mathbf{k}}$. The blue/yellow (black/white) color denotes lower/higher strength. Panel (d) is the MDC along the nodal direction in the normal state with the energy from 0 to -1 eV. Panel (e) shows the energies (E_0, E_1, E_2) vs the scattering intensity V in the normal state.

case, and H_C is the term that represents the charge modulation,

$$H_C = \sum_{\mathbf{Q}\mathbf{k}\sigma} (V c^{\dagger}_{\mathbf{k}+\mathbf{Q}\sigma} c_{\mathbf{k}\sigma} + \text{H.c.}), \tag{3}$$

where $\mathbf{Q}$ are the scattering wave vectors. Hereafter, the related parameters are chosen as $t=0.35$ eV and $t'=-0.25t$. The chemical potential μ is determined by the doping density $\delta=0.12$. We here use the isotopic s-symmetry modulation with the wave vectors $\mathbf{Q}=(0,2\pi/4)$ and $(2\pi/4,0)$ and the intensity $V=0.1$ eV.[26] We have examined that our results are not sensitive to the slight changes of the chosen parameters and the robustness of our main conclusion with respect to the scattering intensity V.

The electronic spectral function is given by $A(\mathbf{k},\omega) = -1/\pi \, \text{Im}\, G(\mathbf{k},\omega+i\Gamma)$, where the retarded Green's function $G(\mathbf{k},\omega+i\Gamma)$ is obtained by diagonalizing the Hamiltonian [Eq. (1)]. The intensity plots of $A(\mathbf{k},\omega)$ are presented in Figs. 1(a)–1(c). We also plot the bare quasiparticle dispersions $\varepsilon_{\mathbf{k}}$ in the absence of the modulation (the solid white lines) as a function of the momentum $\mathbf{k}$ for comparison. As seen, at low energies, the quasiparticle dispersions coincide almost with the bare ones, while they deviate from the bare ones when the momentum is close to $\mathbf{K}_0=(\pi/4,\pi/4)$. Then, they break up at the energy $E_1 \approx -0.35$ eV around the momentum $\mathbf{K}_0$ and the quasiparticles would be ill defined within $E_1 < E < E_2$. At the energy $E_2 \approx -0.75$ eV, the dispersions reappear and disperse toward the (0,0) point. These results are independent on the SC order, as seen in Figs. 1(b) and 1(c). The momentum distribution curves (MDCs) for different energies are plotted in Fig. 1(d). Two dispersive bands are revealed at the low and high energies, respectively. Moreover, we can clearly see from Fig. 1(c) that the peaks of MDC are weakly dispersive between the energies E_1 and E_2, i.e., nearly pinned at the momentum $\mathbf{K}_0$ with lower intensity, consistent with the experimental results.[8–14] E_1 and E_2 as a function of the scattering intensity V are plotted in Fig. 1(e), where E_0 is the bare quasiparticle energy at the momentum $\mathbf{K}_0$. E_1 and E_2 approach to E_0 as V decreases to zero; E_1 decreases and E_2 increases almost linearly when V increases. The main results are more robust as V changes slightly.

A sound explanation for the described anomalous higher-energy features can be given based on the following scattering characteristic illustration. The first Brillouin zone as well as the normal-state Fermi surface are presented in Fig. 2(a). As seen, the Brillouin zone may be divided into 16 parts in the presence of the modulation term, labeled as 1 to 16. When the modulation term acts on an electron in part i, it makes the electron hop to the four neighboring parts.[27] Let us assume that an electron at A_0 in region 1 has the momentum (k,k) (i.e., along the diagonal direction). The effect of the modulation term makes it hop to A_{1-4} in the neighboring regions 8,4,2,11, respectively, as shown in Fig. 2(a). The corresponding momenta for the electrons at A_{1-4} are $(k-\pi/2,k),(k,k+\pi/2),(k+\pi/2,k),(k,k-\pi/2)$, respectively. We present the bare dispersions for $A_i (i=0-4)$ in Fig. 2(b). The dispersions for the electrons at A_1 and A_4 (or A_2 and A_3) coincide because they are symmetric points. We can see from Fig. 2(b) that the quasiparticle energy at A_0 is different from that at A_i as the momentum is far from $\mathbf{K}_0$. Thus, the hopping from A_0 to A_i is difficult to occur because the energy conservation condition is not satisfied. As a result, the modulation has little effect on the hopping for this case, namely, the quasiparticle is well defined and the dispersion coincides almost with the bare one, as shown in Fig. 1(a). When the momentum decreases and moves close to $\mathbf{K}_0$, the energy at A_0 is closer to that at A_1 and A_4. The charge modulation influences the dispersion significantly. Thus, it deviates from the bare one and the spectral weight reduces gradually. When the momentum reaches $\mathbf{K}_0$, the bare quasiparticle energy at A_0 just equals to that at A_1 and A_4, as seen in Fig.

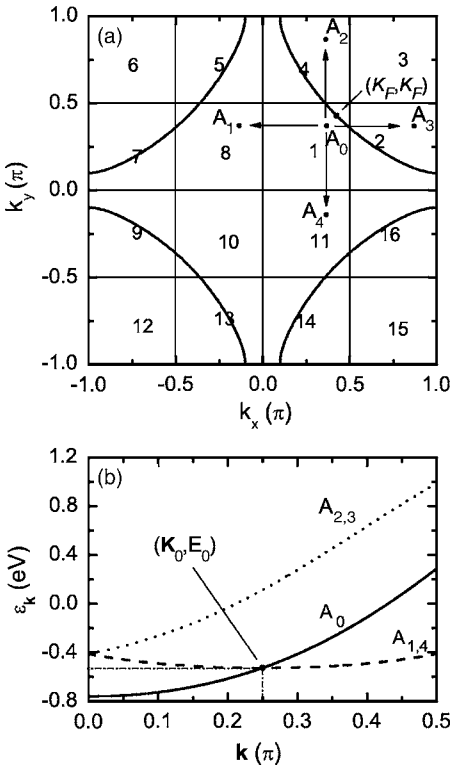

FIG. 2. (a) The first Brillouin zone as well as the normal-state Fermi surface, with the scattering from A_0 to A_i indicating the hopping caused by the charge modulation term. (b) The bare dispersion of quasiparticles at A_0 (along the diagonal direction) and the corresponding dispersions of that at A_i.

2(b), so that the hopping from A_0 to $A_{1,4}$ can occur easily, which destroys the state of the quasiparticle at A_0 and leads the dispersion to break up at this momentum. As a result, the dispersion is pinned by the modulation term and the quasiparticle is ill defined. On the other hand, the quasiparticle dispersion is no longer pinned by the modulation when the bounding energy is high enough (larger than E_2), and thus it reappears and disperses toward (0,0) point. In fact, when the electron leaves the $\mathbf{K}_0$ point, the energy at A_0 is different from that at A_i and thus the quasiparticle is well defined again.

In the SC state, the quasiparticle energy at A_0 is the same as that in the normal state along the diagonal direction, while that at A_i is changed due to the presence of the SC gap. Meanwhile, the quasiparticle energy at A_0 equals that at $A_{1,4}$ at the momentum $\mathbf{K}_0$ because $A_{1,4}$ is along the nodal direction at this momentum. Thus the addressed anomaly depends weakly on the SC order parameter Δ_0. The spectra in the d-wave SC state are almost the same with those in the normal state. In the s-wave SC state, a clear gap can be seen and the corresponding anomalous energy E_i is a little larger than that in the normal state, while the SC gap is much smaller than the energies $E_{1,2}$; thus, in fact, the spectra are also similar with those in the normal and d-wave SC states.

It is expected that the anomaly would occur at a fixed momentum $\mathbf{K}_0=(\pi/4,\pi/4)$ in terms of the present scattering wave vector $\mathbf{Q}$, which, in fact, corresponds to the four-unit-cell modulation observed in the STM results as mentioned above. This is well consistent with an earlier experimental report that the dispersion is found to break up at roughly the momentum $(\pi/4,\pi/4)$.[8] More recently, it is also suggested by Valla *et al.* that the anomaly may occur at different momenta, depending on the systems and doping,[10] as revealed likely in some experiments that the modulation is not fixed to be the four-unit-cell.[6] In this sense, the momentum K_0 could also vary as the scattering wave vector changes. In addition, although here we give a possibility that the charge modulation may be responsible for the higher-energy anomaly, the model is merely primitive and phenomenological. In the present model, other possible interactions, such as the effects of the phonon, spin fluctuation, or plasmon, have been neglected, as we believe that they are unlikely the main reason of the anomaly. Certainly, they may still play some important roles in obtaining the quasiparticle dispersion quantitatively. Clearly, here we merely attempt to explain the experiments qualitatively, while a more rigorous model is still awaited for quantitative comparisons with the ARPES and STM experiments.

On the other hand, it is still unclear whether similar charge modulation also emerges in the electron-doped superconductors. If such modulation is present, it is anticipated that the anomaly will also appear correspondingly. In addition, the Fermi momentum K_F along the diagonal direction [shown in Fig. 2(a)] is larger in the electron-doped ones.[18] As a result, the bare bounding energy E_0 at the momentum $\mathbf{K}_0$ is larger than that of the hole-doped one. From the above-presented picture, the corresponding anomalous energies are also larger than those for the hole-doped ones, which may be consistent with the experimental results.[13,14]

We now turn to address the FT-STM spectra. As we mentioned above, the FT-STM spectra can be related to the ARPES spectra through the AC-ARPES function $C(\mathbf{q},\omega)$, given by[20]

$$C(\mathbf{q},\omega)=\frac{1}{N}\sum_{\mathbf{k}}A(\mathbf{k},\omega)A(\mathbf{k}+\mathbf{q},\omega). \tag{4}$$

Very recently, it was concluded experimentally that the FT-STM spectra are in good agreement with the AC-ARPES spectra at low energies for various doping densities.[21] Therefore, we are able to relate the obtained ARPES results to the STM spectra by using the AC-ARPES function to deduce the FT-STM spectra and compare the results with the STM experiments. The calculated intensities of the AC-ARPES spectra at zero energy, in the normal and SC states, are shown in Figs. 3(a) and 3(b), respectively. The logarithmic scale is used so that the weak features can be revealed. As shown, four peaks appear at the momenta $(\pm 2\pi/4,0)$ and $(0,\pm 2\pi/4)$. These peaks are independent of the energies, as seen more clearly in Figs. 3(c) and 3(d), which are the two-dimensional cuts of the spectra for the energies from −0.02 to 0.02 eV. These nondispersive peaks in the FT-STM spectra were observed experimentally in the normal state.[2] In the SC state, while they are suppressed by the SC order, they were also indeed observed by STM experiments as well.[3–6]

The consistency between the FT-STM and AC-ARPES spectra indicates that the nondispersive peaks may be ex-

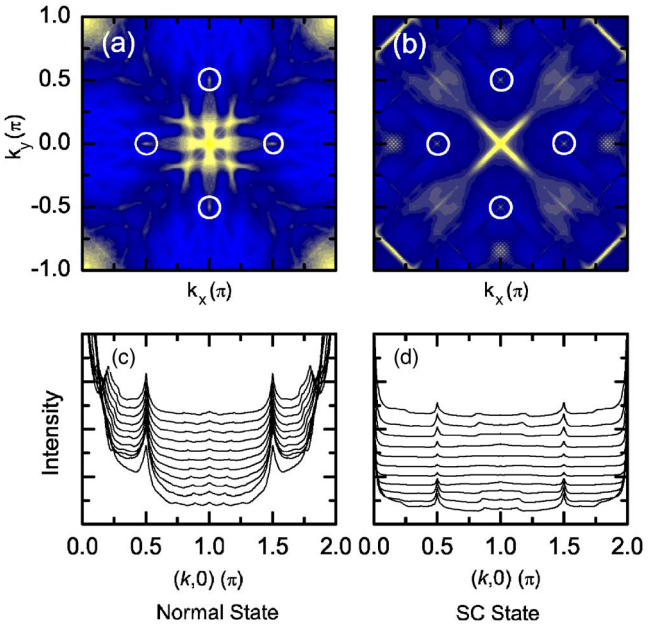

FIG. 3. (Color online) Panels (a) and (b) are the intensity plots of the AC-ARPES spectra $C(\mathbf{q},\omega)$ at the zero energy in the normal and SC states (Δ_0=0.04 eV), respectively. Circles are used to denote the energy-independent peaks. Panels (c) and (d) are the two-dimensional cuts for the spectra along (0,0) to $(2\pi,0)$ with the energy increasing from −0.02 to 0.02 eV (from the bottom to the top) in the normal and SC states, respectively.

plained based on the quasiparticle interference model;[28,29] i.e., the momenta of the peaks in FT-STM spectra are just the wave vectors that connect the tips of the constant energy contour. Based on this picture, the various dispersive peaks observed by STM experiments in the SC state[28,30] are reproduced successfully. At present, in the presence of the charge modulation, the intensity plots of the ARPES spectra at zero energy are depicted in Fig. 4(a) for the normal state and in Figs. 4(b) and 4(c) for the SC state; since the ARPES spectrum is reduced to a dot along the nodal direction in the SC state [Fig. 4(b)], we replot it by using a logarithmic scale in Fig. 4(c) to reveal the weak features caused by the charge modulation. As we discussed above, the ARPES spectra break up at the momenta $\mathbf{K}_i=(\pm\pi/4,q)$ and $\mathbf{K}_i'=(q,\pm\pi/4)$ because of the modulation, leading to the tips of the spectra at these momenta. In the corresponding AC-ARPES spectra, the peaks appear at the momenta $\mathbf{Q}_i$ that connect the tips of the ARPES spectra, as denoted in Figs. 4(a) and 4(c). As a result, although the charge modulation has a very weak effect on the low-energy ARPES spectra, which is difficult to be detected directly by the ARPES experiments, the nondispersive peaks induced by the modulation appear clearly in the AC-ARPES spectra (or the FT-STM spectra) and can be detected firmly by the STM experiments.

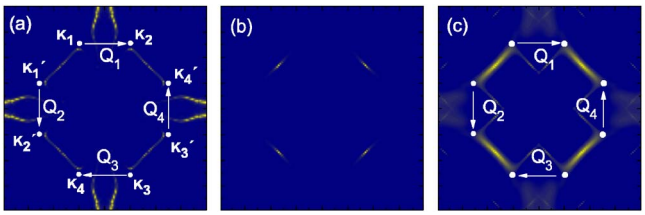

FIG. 4. (Color online) Panels (a) and (b) are the intensity plots of ARPES spectra at zero energy in the normal and SC states, respectively. Panel (c) is the replotting of the spectra in the SC state where the logarithmic scale is used.

To conclude, based on a phenomenological model, we have elaborated that the rotationally symmetric charge modulation is able to cause the intriguing dispersion anomaly observed in the ARPES spectra as well as the nondispersive peaks in the FT-STM spectra. A clear physical picture of the mechanism was presented based on the scattering analysis in the presence of the charge modulation.

We thank Y. Chen, L. H. Tang, and Q. H. Wang for helpful discussions. This work was supported by the RGC grants of Hong Kong (HKU 7050/03P and HKU-3/05C), the NSFC (10429401), and the 973 project of China (2006CB601002).

[1] J. E. Hoffman *et al.*, Science **295**, 466 (2002).
[2] M. Vershinin *et al.*, Science **303**, 1995 (2004); T. Hanaguri *et al.*, Nature (London) **430**, 1001 (2004).
[3] C. Howald, H. Eisaki, N. Kaneko, M. Greven, and A. Kapitulnik, Phys. Rev. B **67**, 014533 (2003).
[4] A. Fang, C. Howald, N. Kaneko, M. Greven, and A. Kapitulnik, Phys. Rev. B **70**, 214514 (2004).
[5] A. Hashimoto, N. Momono, M. Oda, and M. Ido, Phys. Rev. B **74**, 064508 (2006).
[6] K. McElroy, D. H. Lee, J. E. Hoffman, K. M. Lang, J. Lee, E. W. Hudson, H. Eisaki, S. Uchida, and J. C. Davis, Phys. Rev. Lett. **94**, 197005 (2005).
[7] D. Zhang, Phys. Rev. B **66**, 214515 (2002); D. Podolsky, E. Demler, K. Damle, and B. I. Halperin, *ibid.* **67**, 094514 (2003); S. Sachdev and E. Demler, *ibid.* **69**, 144504 (2004); J. X. Li, C. Q. Wu, and D.-H. Lee, *ibid.* **74**, 184515 (2006).
[8] J. Graf *et al.*, Phys. Rev. Lett. **98**, 067004 (2007).
[9] B. P. Xie *et al.*, Phys. Rev. Lett. **98**, 147001 (2007).
[10] T. Valla *et al.*, cond-mat/0610249 (unpublished).
[11] J. Graf, G.-H. Gweon, and A. Lanzara, cond-mat/0610313 (unpublished).
[12] J. Chang *et al.*, cond-mat/0610880 (unpublished).
[13] Z.-H. Pan *et al.*, cond-mat/0610442 (unpublished).
[14] W. Meevasana *et al.*, cond-mat/0612541 (unpublished).
[15] F. Ronning, K. M. Shen, N. P. Armitage, A. Damascelli, D. H. Lu, Z. X. Shen, L. L. Miller, and C. Kim, Phys. Rev. B **71**, 094518 (2005).
[16] M. Eschrig and M. R. Norman, Phys. Rev. Lett. **89**, 277005 (2002); T. Cuk *et al.*, *ibid.* **93**, 117003 (2004); J. X. Li, T. Zhou, and Z. D. Wang, Phys. Rev. B **72**, 094515 (2005).
[17] A. M. Gabovich, A. I. Voitenko, and M. Ausloos, Phys. Rep. **367**, 583 (2002); S. A. Kivelson *et al.*, Rev. Mod. Phys. **75**, 1201 (2003).
[18] A. Damascelli, Z. Hussain, and Z.-X. Shen, Rev. Mod. Phys. **75**,

473 (2003).
[19] K. M. Shen *et al.*, Science **307**, 901 (2005).
[20] R. S. Markiewicz, Phys. Rev. B **69**, 214517 (2004).
[21] K. McElroy, G. H. Gweon, S. Y. Zhou, J. Graf, S. Uchida, H. Eisaki, H. Takagi, T. Sasagawa, D. H. Lee, and A. Lanzara, Phys. Rev. Lett. **96**, 067005 (2006).
[22] Q. H. Wang, F. Tan, and Y. Wan, cond-mat/0610491 (unpublished).
[23] Z. Islam *et al.*, Phys. Rev. Lett. **93**, 157008 (2004).
[24] J. M. Tranquada *et al.*, Nature (London) **375**, 561 (1995); Phys. Rev. Lett. **78**, 338 (1997); K. Yamada *et al.*, Phys. Rev. B **57**, 6165 (1998); A. Lucarelli *et al.*, Phys. Rev. Lett. **90**, 037002 (2003); T. Noda, H. Eisaki, and Shin-ichi Uchida, Science **286**, 265 (1999); X. J. Zhou *et al.*, *ibid.* **286**, 268 (1999).
[25] K. Machida, Physica C **158**, 192 (1989); J. Zaanen and O. Gunnarsson, Phys. Rev. B **40**, 7391 (1989); V. J. Emery and S. A. Kivelson, Physica C **209**, 597 (1993); V. J. Emery, S. A. Kivelson, and J. M. Tranquada, Proc. Natl. Acad. Sci. U.S.A. **96**, 8814 (1999); K. Machida and M. Ichioka, J. Phys. Soc. Jpn. **68**, 2168 (1999); J. M. Tranquada, J. Phys. IV **131**, 67 (2005); Proc. SPIE **5932**, 59320C (2005); E. Arrigoni, E. Fradkin, and S. A. Kivelson, Phys. Rev. B **69**, 214519 (2004); M. Raczkowski, A. M. Oles, and R. Fresard, Low Temp. Phys. **32**, 305 (2006).
[26] A further study for the symmetry of the charge order may agree better with experiments, while it is not a main concern of the present paper. We have also checked numerically that the real-space modulations observed by the STM experiments (Ref. 2) can be reproduced likely (not shown here) with the present model and chosen parameters.
[27] Taking into account the periodicity in the momentum space, the parts that include the border of the Brillouin zone, such as parts 2 and 7, are also seen as the neighbor parts.
[28] K. McElroy *et al.*, Nature (London) **422**, 592 (2003).
[29] Q. H. Wang and D.-H. Lee, Phys. Rev. B **67**, 020511(R) (2003).
[30] J. E. Hoffman *et al.*, Science **297**, 1148 (2002).